ELSEVIER

Journal of Power Sources 74 (1998) 99–107

JOURNAL OF POWER SOURCES

Studies of activated carbons used in double-layer capacitors

Deyang Qu *, Hang Shi [1]

Emtech, 2486 Dunwin Drive, Mississauga, ON, Canada L5L 1J9

Received 15 December 1997; accepted 12 January 1998

Abstract

Various kinds of activated carbon materials were investigated by means of nitrogen gas adsorption, AC impedance and constant current discharge techniques. The relation between the intrinsic pore size distribution of activated carbon materials and their electrochemical performance as electrodes of supercapacitor were discussed in detail. Activated carbons with larger pores are found to be more suitable for high power applications. The electrochemical accessible time to pores of various sizes obtained from the fitting of AC impedance data was successfully correlated with the pore size distribution of the materials. © 1998 Elsevier Science S.A. All rights reserved.

Keywords: Activated carbon; Supercapacitor; Pore size distribution; High rate; Pore accessibility

1. Introduction

There is growing interest in the use of electrical/electrochemical energy storage systems under condition in which the electrical power output is highly time-dependent, or in other words, short-term pulse. These output characteristics are different from those of conventional battery systems that can be considered as devices of lower power levels. Great attention is then focused on electrochemical supercapacitor/ultracapacitor energy-storage systems in recent years on account of possible application in electric vehicles and any device that need high-pulse discharge profile, e.g., digital telecommunication systems [1–10]. Electric double-layer capacitors have already been used as memory backup systems for almost a decade in many fields of electric equipment such as videocassette recorder, typewriter, personal organiser, etc. [11].

A unit cell of double-layer capacitor is based on the double-layer capacitance at the solid/solution interface of high-surface area material e.g., activated carbon. Similar to a traditional electrolytic capacitor, the electrical energy is stored based on the separation of charged species in an electrolytic double-layer across the interface of electrode/solution.

Helmoholtz in 1879 [12], Gouy in 1910 [13,14], Chapman in 1913 [15] and Stern [16] in 1924 discovered that charges can be separated and form a double layer cross a conductor and a liquid electrolyte. The interface models [17] were further established to explain the phenomenon of the double layer. When DC voltage is applied to the interface of an electrode, electric double-layer is then established to store electric energy. The electric capacitance stored in the layer is proportional to the surface area of the electrode and $\frac{1}{\text{thickness}}$ of the double layer. In strong and concentrated electrolyte solution, a double layer has a thickness of only a few angstroms. By choosing a suitable high surface area material, e.g., certain activated carbons with BET surface area of more than 1000 m^2/g, a practical 'supercapacitor' with specific capacitance, e.g., 120 F/g of carbon can be possibly engineered with proper techniques of electrode fabrication.

An electric double-layer capacitor (EDLC) is a device that consists of a pair of ideally polarizable electrodes; in other words, only devices that do not exhibit Faradic reaction over the potential range of operation are considered EDLCs, and all the charges accumulated are used to build-up a double layer between the conductor/solution. Some insignificant side reactions that involve Faradic charge transfer could happen in the potential range of the operations; for example, the redox reaction of impurities: these kinds of Faradic reactions can be considered as self-discharge reaction of supercapacitors because charges accumulated cross the interface will be consumed in those

* Corresponding author. Rayovac, 601 Rayovac Drive, Madison, WI 53719, USA.

[1] Current Address: Valence Technology, 301 Conestoga Way, Henderson, NV 89015, USA.

0378-7753/98/$19.00 © 1998 Elsevier Science S.A. All rights reserved.

Petitioner Intel Corp., Ex. 1048
IPR2023-00783

reactions, and total amount of the charges in the double-layer will decrease [18]. Thus, side Faradic reactions that are mostly the redox reaction of impurities in the solution and functional groups on the carbon surface should be avoided. Charge and discharge of an EDLC, in fact, is charge and discharge of the double layer, because no electrochemical reaction is involved. Therefore, the reversibility of an EDLC is much better than any secondary battery. Practically, the limitation of the cycle life of an electrochemical double-layer capacitor is due to the engineering of the devices rather than its chemistry as that in secondary batteries.

Recently, Conway [19] discussed the transition from 'supercapacitor' to 'battery behaviour' in electrochemical energy storage. A 'battery-like' supercapacitance based on Faradic pseudocapacitance of redox reaction at two-dimensional electrode surface and quasi two-dimensional or three-dimensional in microporous transition metal hydrous. The pseudocapacitance of two-dimensional redox resulted from underpotential deposition. Due to the thermodynamics of the electrode/electrolyte interface, underpotential deposition of, e.g., H or Pb in monolayer on the noble metals can occur before the 3-D bulk deposition of new phase happens, so the surface of the electrode is partially covered; thus, an 'electrosorption pseudocapacitance' of about 200–400 mF/cm^2 can be achieved. The pseudocapacitiance based on three-dimensional Faradic reaction results from the 'super-reversible' redox reaction in microsporous transition metal hydrous, e.g., RuO_2 or IrO_2.

In the family of the 'supercapacitor' based on the theory of 'pseudocapacitance', the principal of using intercalation compounds was also discussed [20]. The supercapacitor based on intercalation, most probably Li-intercalation, includes two electrodes made with the same type of intercalation material, e.g., $LiMn_2O_4$ spinel in the non-aqueous [21] or aqueous [22] electrolyte. The theory of such kind of 'supercapacitor' is similar with that of 'Li-ion' or 'Rocking-chair' batteries, but instead of using two different types of intercalation materials as anode and cathode, e.g., carbon and $LiMn_2O_4$, respectively, in a Li-ion battery, the same intercalation material is used for both electrodes in a 'supercapacitor'. During charge and discharge of the capacitor, Li^+ ions are shuttling between the two electrodes. During discharge, lithium ions are released from one electrode host structure and inserted into another electrode's host with concomitant oxidation and reduction process taking place at the both electrodes. The reverse processes occur during charging. However, in a 'supercapacitor' device, only half of the Li can be utilised, thus the specific capacity of the material in terms of mAh/g is only half of that in Li-ion batteries. The amount of energy stored (charges $\times$ cell voltage) is proportional to the amount of Li species that can be intercalated into the host electrode, and therefore is reduced to half of that in Li-ion battery as well. Since the intercalation can be treated as a homogeneous reaction mechanism, the discharge curve of such device will be a linear and 'capacitor-like' straight line. The slope of which line relies on the kinetics of the specified intercalation reaction and the maximum voltage of device is dependent on the amount of Li that the host material can accommodate and the 'electrochemical window' of the electrolyte used.

The devices based on 3D Faradic reaction are normally utilised in energy-sensitive pulse application. Because on one hand, the charge storage mechanism can lead to much higher volume of energy per unit volume of the electrodes than those on the surface-related process, but on the other hand, kinetic behaviour of such devices is related to, not only the electrode/electrolyte interface area, but also the kinetic of the Faradic reaction that depends on the activation energy of the charge transfer processes; therefore, the rate capability of such devices cannot be expected to be as high as those based on 2D processes.

The supercapacitors concerned in this paper are EDLC. The Faradic reactions occurred are considered as undesired side-reactions.

2. Experiments

2.1. Materials

Activated carbons were obtained from Spectracorp (USA). Activated carbon powders with different surface area and pore size distribution were used. The precursors of these activated carbon powder are mesophase microbeads.

2.2. Electrolyte, reference and counter electrode

Thirty percent aqueous potassium hydroxide solution was used as the electrolyte in all experiments at a temperature of 298 $\pm$ 1 K. All potentials reported, unless otherwise specified as the voltage of two electrode systems, are referred to the HgO/Hg reference electrode immersed in KOH of the same concentration as the experimental electrolyte. A Ni-mesh was used as counter electrode.

2.3. Construction of the electrodes used in the experiments

Activated carbon of various types was individually mixed thoroughly with LONZA graphite (KS44), respectively at desired ratio using high-speed electric coffee grinder for 10 min, 0.5 wt.% (dry material) of a Teflon suspension (DuPont T-60) as a binder, the resulting active material (activated carbon–Teflon–graphite) was rolled to form flexible films. The thickness of the film was 0.60 mm. Unless specified otherwise, the electrodes were composed of 99.5% of activated carbon and 0.5% of Teflon binder. The electrode used in the experiments were punched out of the big sheet, and the disc electrodes were then mounted onto a Ni-current collector in a Teflon cell holder

Petitioner Intel Corp., Ex. 1048
IPR2023-00783

by means of a screw-fitting plug. If a two-electrode system was used, two disc electrodes of the same type and same size (from the same sheet) were mounted face-to-face into the holder with a non-woven separator in between. Before the electrochemical measurements were conducted, all electrodes were vacuum-wetted.

2.4. Experimental techniques and instrumental details

Constant current charge and discharge was carried by means of Solaritron Electrochemical Interface 1255 controlled by Corrware; AC impedance measurements were conducted by means of Solaritron Electrochemical Interface 1255 and Solaritron Frequency Response Analyser controlled by ZPLOT. All the equivalent-circuit fittings for AC impedance were done by homemade software. Micromeritics ASAP 2000 porosity meter was used for the measurement of surface area and porosity, N_2 gas was used as absorbent. A built-in software based on density function theory was used to estimate the pore size distribution of activated carbons.

2.5. Determination of specific capacitance

The specific capacitances reported in literatures were not consistent, mainly due to the experimental methods used to determine them. For the sake of consistency, it is worth specifying the electrochemical technique used in this paper and discussing how to inter-calculate the specific capacitance between 2-electrode and 3-electrode systems.

Fig. 1b shows the double-layer of electrodes used in two-electrode system (2E), which represents a real double-layer supercapacitor device and its equivalent circuit. Fig. 1a shows the double-layer of electrodes used in three-electrode system (3E), which is used in lab cell with reference electrode and its equivalent circuit.

Assuming that the weight of each individual electrodes is m, then

$$C_1 = C_2 = C$$

The capacitance measured for two electrode system is

$$C_{2\mathrm{E}} = \frac{1}{2}C$$

the specific capacitance turns out to be

$$C_{\mathrm{spec-2E}} = \frac{C_{2\mathrm{E}}}{2m} = \frac{1}{4}\left(\frac{C}{m}\right)$$

However, for the three-electrode system, the double-layer capacitance measured was

$$C_{3\mathrm{E}} = C$$

and the specific capacitance is

$$C_{\mathrm{spec-3E}} = \frac{C_{3\mathrm{E}}}{m} = \frac{C}{m}$$

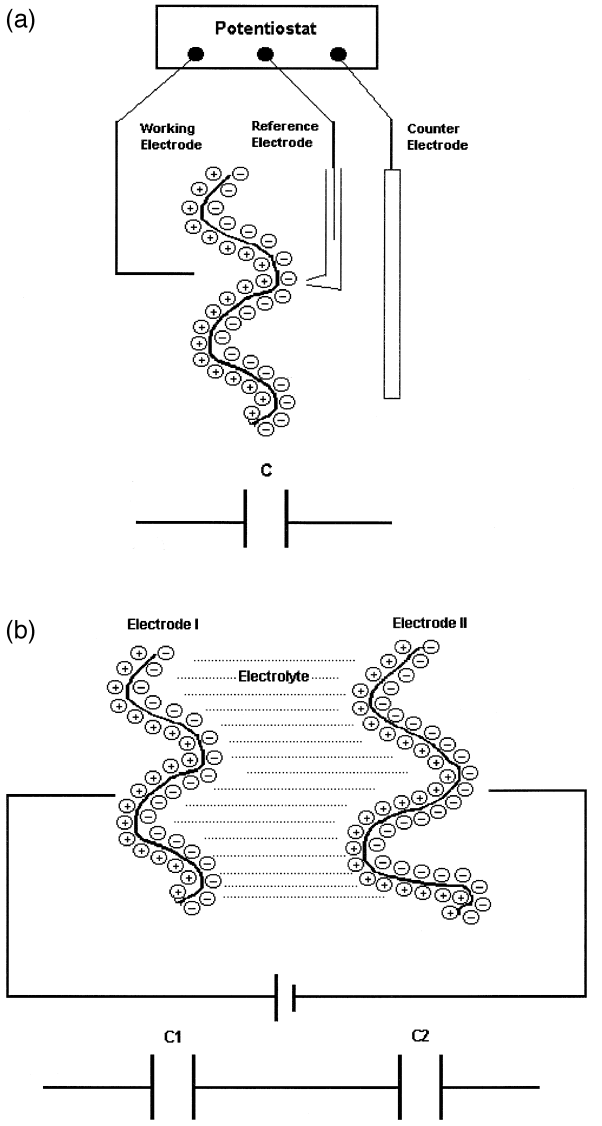

Fig. 1. Electric double layer and its equivalent circuit in 3-electrode system (A) and 2-electrode system (B).

Thus, the relationship between the specific capacitance measured with two-electrode and 3-electrode technique is

$$C_{\mathrm{spec-3E}} = 4 \times C_{\mathrm{spec-2E}}$$

Unless otherwise specified, the specific capacitances reported in this paper were obtained from 3-electrode device and inter-calculated to the 2-electrode system.

It will be shown in the next paper that the measured specific capacitance of a certain material also depends on the electrolyte system (e.g., alkaline, acidic, organic electrolyte) and potential. Unless otherwise specified, the capacitances reported were measured by AC-Impedance technique at OCV in 30% KOH solution.

Petitioner Intel Corp., Ex. 1048
IPR2023-00783

3. Results and discussion

The nature of double-layer capacitor energy storage device is based on storage of electrical energy by change separation at its two electrodes with a developed voltage difference across the electrolyte. The maximum voltage difference is determined by the decomposition potential of electrolyte, e.g., aqueous electrolyte 1.2 V; non-aqueous electrolyte 2–4 V.

The capacitance of a double-layer supercapacitor depends on the surface area of the carbon material used in electrodes. The specific capacitance should be defined as specific surface area of the carbon × specific double layer capacitance (F/cm^2). Theoretically, the higher the specific surface area of an activated carbon, the higher the specific capacitance should be expected. However, practical situations are more complicated. Table 1 tabulates the relationships among the capacitance (f/g) calculated from low-frequency impedance (1 mHz), BET surface area, total pore volume and average pore size of various activated carbons. It is obvious that the measured capacitance of activated carbons did not have a linear relationship with their surface area; in fact, some activated carbons with smaller surface area had larger specific capacitance than those with a larger surface area. There are two primary reasons for the phenomenon: first, the double layer capacitance (F/cm^2) varies with various types of activated carbons that were made from different types of precursor, through different processes and subsequent treatments; second, small diameter micropores may not be accessible to electrolyte solution, simply because ions, especially those ions with hydration shells [23], and big organic ions, are too big to enter those pores; thus, the surface area of those non-accessible micropores will not contribute to the total double-layer capacitance of the material.

The surface area of a given mass of solid material is inversely related to the size of the constituent particles. In practice, the particles of a fine powder, the primary particles [24], will stick together because of the surface forces to form secondary particles. Pores are formed in those aggregated particles. Pore size depends on the size and shape of primary particles and how they are packed together. So the surface area of a solid can be conveniently distinguished between the external and internal surface. External surface includes all the outer surface of secondary particles, and all of those cracks that are wider than they are deep. The internal surfaces will then comprise the walls of all cracks, pores and cavities that are deeper than they are wide. Obviously, external pores are much easier to be accessed by electrolyte than those of internal pores.

In-depth studies have been conducted by Soffer et al. [25] and Koresh and Soffer [26,27], and recently by Shi [28], on the accessibility of micropores to aqueous solutions; it has been concluded that since the size of single N_2 molecule is similar to that of OH^- or K^+ ions in aqueous solution, those micropores that can accommodate adsorbed nitrogen molecules at 77 K are also available for the electro-adsorption of simple hydrated ions at low, concentration-dependent rate. Those authors concluded that in principle, pores whose size were larger then 5 Å can be eventually accessible electrochemically.

The applications of supercapacitor can be divided into two main categories: power supplier and memory backup. The former application needs high (super-high) current drain, e.g., supercapacitor used in electric vehicle application; the later application, however, requires high-energy density at low drain rate, e.g., memory backup capacitor in electronic organizer. Therefore, the material used in different applications should be chosen according to different rules. It is in the scope of this paper to discuss in-depth about material selection for various applications of supercapacitor based on the detailed experimental and theoretical fitting works.

Various carbon materials have unique pore distribution, resulting from the precursor and processes involved. Pores with different sizes have different time constants. Fig. 2 shows the pore size distribution of some activated carbons used in this paper. Also, problems of a different kind arise due to finite resistance of the particles and the supporting electrolyte, and to interparticle contact resistance. All these situations can be roughly represented by an equivalent circuit as shown in Fig. 3, which involves a distributed

Table 1
Comparison of specific capacities, surface area, pore volume and average pore size of activated carbons

Carbon	Specific capacity (F/g)	Specific capacity (F/cm^2)	BET surface area (m^2/g)	Pore volume (cc/g)	Average pore size (Å)
M-10	55.95	0.041	1370	0.500	9.12
M-14	57.20	0.0047	1223	0.561	9.60
M-15A	78.10	0.043	1800	0.629	9.17
M-15B	55.80	0.034	1624	0.563	9.37
M-15C	63.34	0.042	1518	0.600	9.79
M-20	100	0.046	2130	0.709	14.73
M-30	62.9	0.024	2571	1.230	14.95
A-10	35.3	0.031	1150	0.424	–
A-20	41.20	0.020	2012	0.902	14.23
SACF-20	48.8	0.027	1839	0.699	9.74
SACF-25	27.9	0.011	2371	0.977	11.93

Petitioner Intel Corp., Ex. 1048
IPR2023-00783

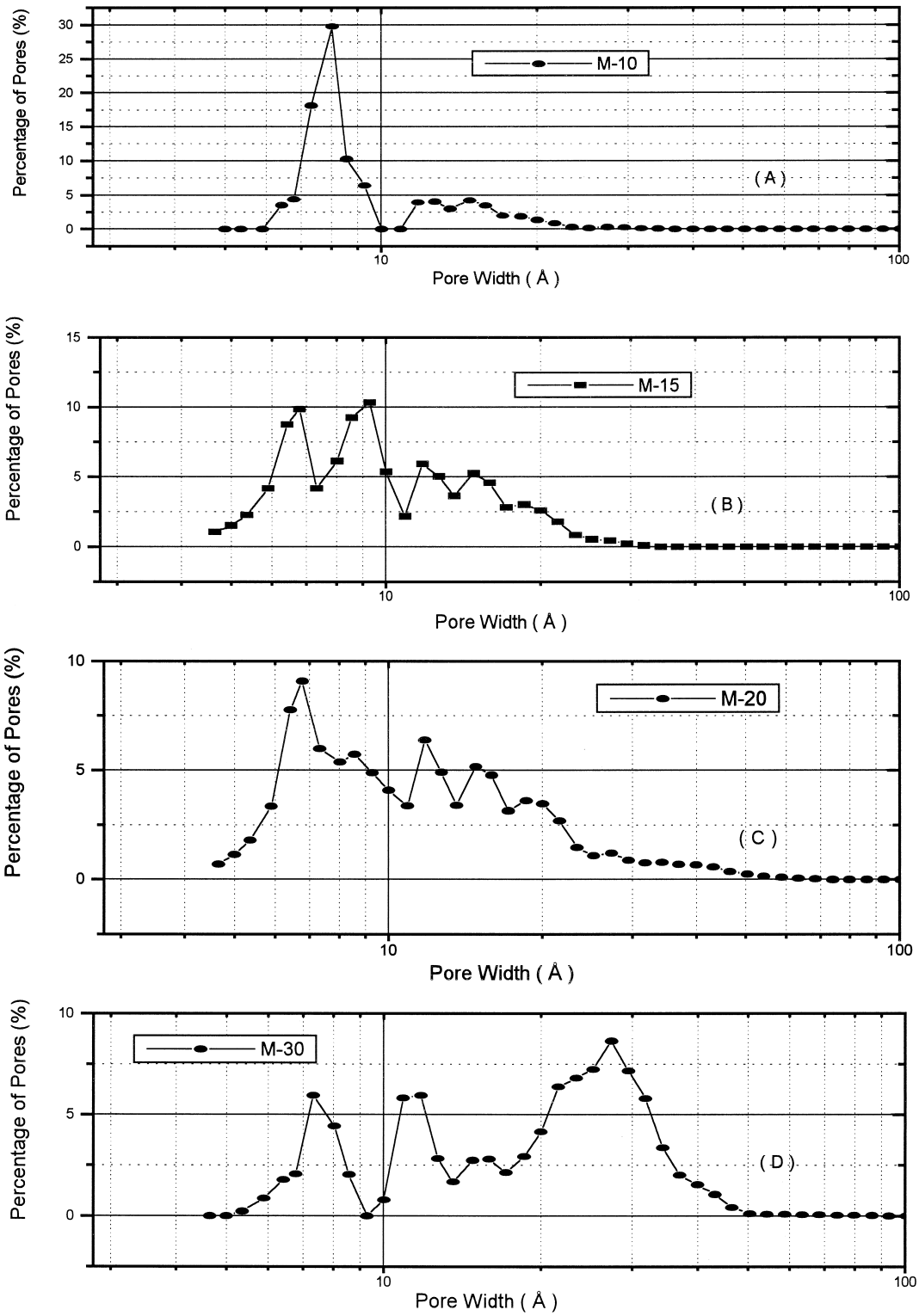

Fig. 2. Comparison of pore size distribution of activated carbons M-10 (A), M-15 (B), M-20 (C) and M-30 (D) calculated from density function theory (DFT).

Petitioner Intel Corp., Ex. 1048
IPR2023-00783

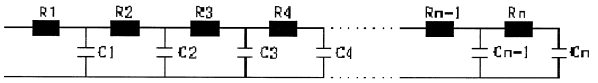

Fig. 3. Transmission line equivalent circuit model used to fit the AC impedance data.

capacitance and resistance, having some of the impedance characteristics of a transmission line. R_i and C_i can be treated as the resistance and capacitance of the pores with certain pore size; R_iC_i which gives the unit of time

$$RC = \left(\frac{V}{I}\right)\left(\frac{It}{V}\right) = t$$

indicates how fast the pore of certain size can be accessed. So, by means of AC impedance and porosity measurements, the electrode made by a carbon material can be well evaluated. Fig. 4 shows the AC impedance spectroscopy, both experimental data and fitting results based on transmission line model shown in Fig. 3. Excellent fitting can be obtained with the transmission line model. Fig. 5 shows the correlations between the time constants (R_iC_i), accumulated capacitance, both obtained from the fitting of AC impedance data (Fig. 5A) and pore size distribution obtained from poresimetry measurements (Fig. 5B). Good correlations can also be seen as established. M-20 and M-30 were used as an example in Fig. 5. The pore-size in Fig. 5B was defined as the surface area of pore opening ($1/\pi r^2$), r was the radius of pore opening. All pores were assumed to be cylindrical. Right axis of Fig. 5B shows the correspondent pore diameters. Fig. 5A shows the electrochemical access time (RC) calculated from the fitting of AC impedance data. What Fig. 5 tells us is that the bigger the pore, the easier and faster being accessed electrochemically. For example, pores with size larger than 11 Å, which represented 25% of the total surface area of M-20, can be electrochemically accessed in less than 0.1 s, while pores with size about 6 Å representing 70% of the total surface area of M-20 can only be accessed for about 5 s. The difference is mainly due to the change of diffusion rate of electrolyte in the pores with different size, and also the network intergrowth with large pores and small pores. The pore network with more larger pores would provide more favorable and quicker pathway for ions to penetrate. In those small pores, local electrical resistance and dielectric constant may be in effect as well. Nevertheless, since bigger pores are earlier to be accessed electrochemically than small pores, those materials with more percentage of big pores should be capable of delivering high power because it can be discharged/recharged at higher current density. However, the surface area of a material is proportional to the total pore volume; the more the amount of small pores, the higher the surface area. If capacitance per square area is assumed to be the same, potentially the

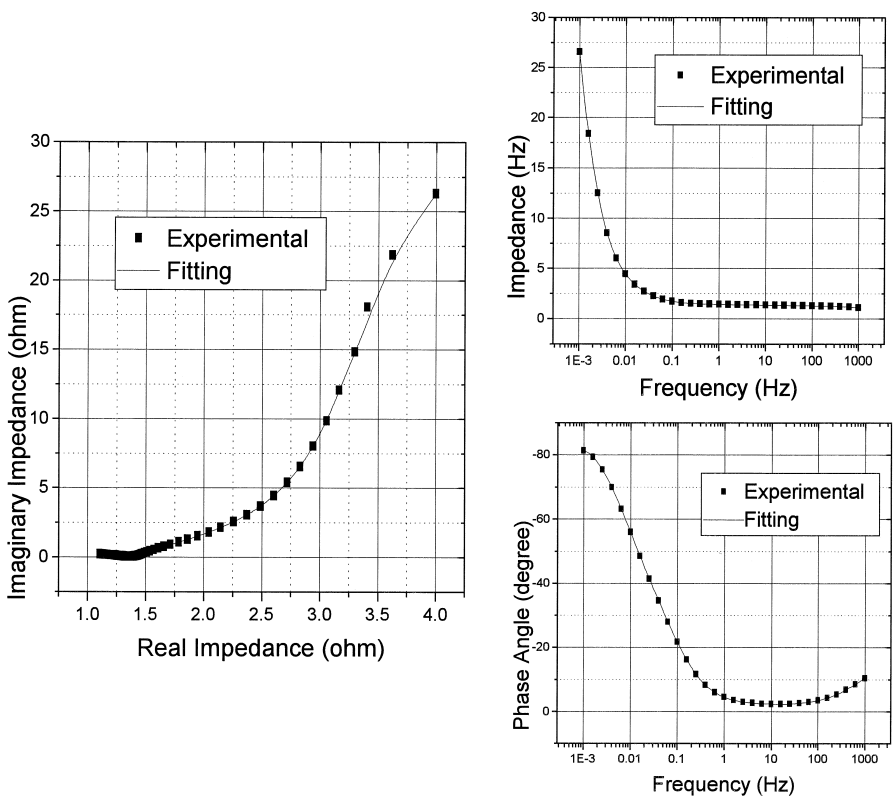

Fig. 4. Comparison of a typical impedance characteristic (complex plane, bode and phase-angle plots) of an activated carbon (M-20) in 3-electrode system at OCV, experimental (■ ■ ■ ■) and fitting (−).

Petitioner Intel Corp., Ex. 1048
IPR2023-00783

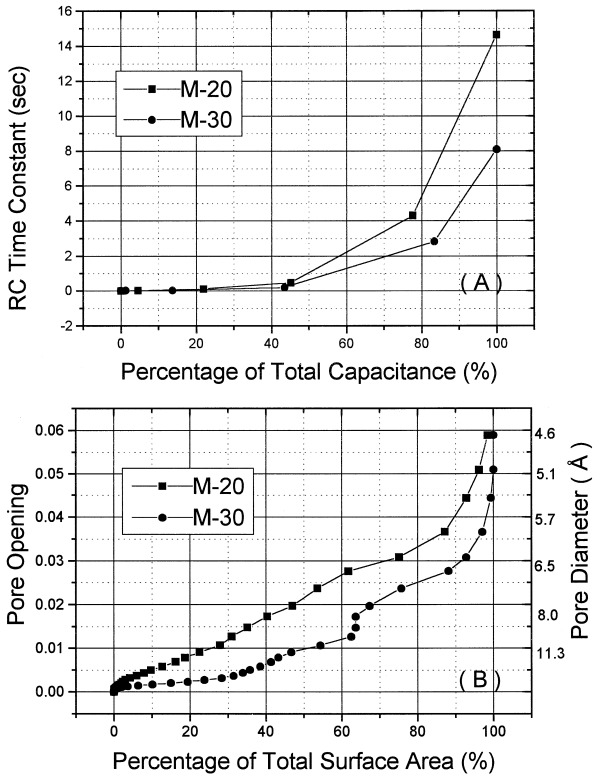

Fig. 5. Comparison of the relation between RC time constant and percentage of total capacitance obtained from fitting of AC impedance (A), the relation between pore size and percentage of total surface area estimated by DFT of M-30 and M-20. Pore opening in (B) was defined as $1/\pi r^2$, r: radius of pore.

higher the gravimetric specific capacitance of the material should occur on materials with smaller pores. Therefore, it is always a trade-off between power density and energy density. The above discussion is based on simplified theoretical approach: every case has to be evaluated on an individual basis.

Fig. 6 shows the relationship between the percentage of total capacitance and the times needed to access them for M-10, M15, M-20 and M-30 based on the fitting of AC impedance data according to the transmission line model.

It should be a good example to compare the pore size distribution and electrochemical accessibility between M-15 and M-20. The surface specific capacitance of M-15 and M-20 were similar, referring to Table 1; they were 0.047 F/cm^2 and 0.046 F/cm^2, respectively. The pore size distribution of M-15 and M-20 are shown in Fig. 2B,C, respectively. The percentage of pores larger than 10 Å were similar between these two. The size of most of the small pores are between 6 Å and 7 Å in both cases. However, M-15 has an additional peak at pore size of 9 Å in Fig. 2b; it means that the percentage of pores with a pore size about 9 Å is higher in M-15 than in M-20. Referring to Fig. 5, one can realise that those pores with size larger than 8 Å can be electrochemically accessed

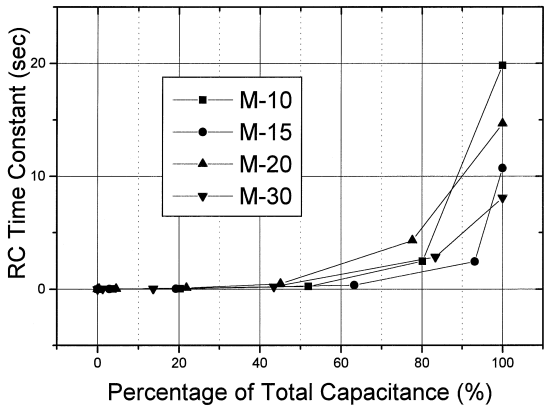

Fig. 6. The relation between RC time constants and percentage of total capacitances of M-10, M-15, M-20 and M-30.

rather quickly. The access time of those pores represents the initial flat region of Fig. 5A, and is less than 2 s. So, although the surface area of M-15 was smaller than that of M-20, the total capacitance of M-15 was lower; thus the total energy stored in per unit weight of M-15 was lower, the deliverable energy of M-15 at high current drain rate would be higher than that of M-20, due to the distribution of more easily accessible pores and network in M-15. Fig. 7 shows the relationship between the deliverable specific capacity (mA h/g) and the current density (mA/g). At the lower current drain rate, both M-20 and M-15 delivered almost theoretical capacity of each material, because of the higher specific surface area of M-20 and similar surface specific capacitance (F/cm^2), M-20 had higher capacity at low drain rate; however, as the discharge current increased, the deliverable capacity M-20 declined much more rapidly than that of M-15. The crossover region was at about 800 mA/g rate. At 3 A/g discharge rate, the discharge capacity of M-15 was more than twice as that of

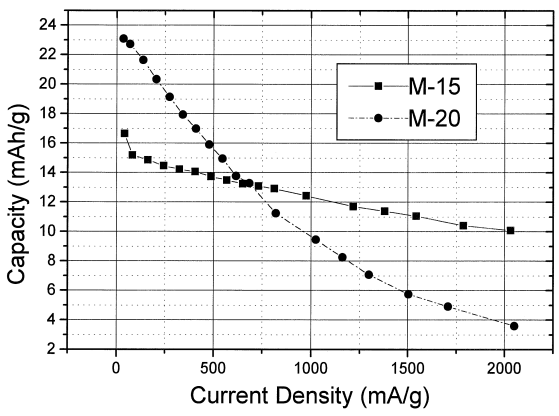

Fig. 7. The relationship between discharge capacity (mA h/g) and discharge current density (mA/g) of 2-electrode supercapacitor made by M-15 and M-20.

Petitioner Intel Corp., Ex. 1048
IPR2023-00783

M-20. The results from this 'real-life' discharge experiments were in good agreement with the results obtained from the fitting of AC impedance data (Fig. 6) based on the transmission line model (Fig. 3). Fig. 6 shows more than 90% of the total capacitance of M-15 (70 F/g) can be electrochemically accessed rather quickly, while only less than 60% of the total capacitance of M-20 (60 F/g) can be accessed at the same rate.

As mentioned previously, a supercapacitor can be used as either energy storage devices, e.g., memory backup application, or as power storage devices, e.g., electric vehicle application. The energy stored in M-20 obviously was higher than that in M-15, due to the high surface area of the material; it made M-20 a more desirable porous material for those applications that require not only high cycle-life but also high reliability at low discharge rate; however, if the demand is high power, M-15 was definitely a better option than M-20, because of its ability of releasing more energy at high drain rate.

Another more complex example would be the comparison of M-20 with M-30. Fig. 8 shows the constant current discharge of electrodes made by M-20 and M-30 at different current densities. M-20 showed higher discharge capacity at low rate, and the capacity declined rapidly as discharge current risen than that of M-30, although the M-30 showed lower capacity at low rate than M-20. Comparing the pore distribution of M-30 and M-20 in Fig. 2, a conclusion can be made that M-30 had much more favourable pore distribution for high rate discharge. The size of the majority of pores in M-30 activated carbon were about 10 Å and a large portion of those pores were even larger than 100 Å, which are in the range of mesopores. Those pores are very easily accessible by electrolyte electrochemically. On the other hand, the majority of M-20 pores were smaller than 10 Å. As discussed previously, the power density of a double-layer capacitor made by porous electrodes is dictated largely by the pore distribution of its electrode material. Fig. 5A shows how fast a certain percentage of total capacitance of M-20 and M-30 can be electrochemically accessed; Fig. 5B shows the relation between percentage of total surface area and the size of pores. In a good agreement with those predicted based on pore distribution (Fig. 2), fitting of AC impedance (Fig. 5A) shows M-30 can indeed be accessed faster than M-20 electrochemically. Comparing Fig. 5A and Fig. 5B, a good correlation between the results obtained from AC impedance fitting and those from porosity measurements can be established. In addition, both AC impedance fitting and pore distribution data are consistent with those results obtained from constant current discharge (Fig. 8) again.

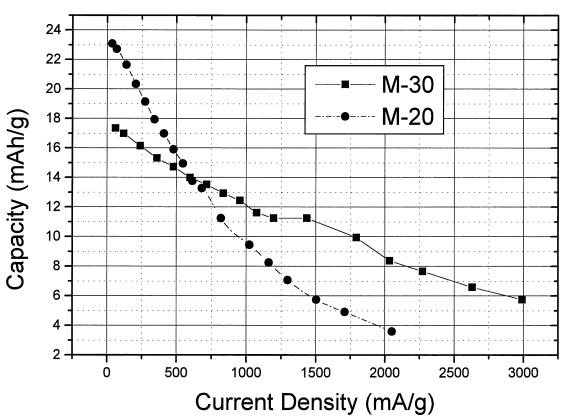

Fig. 8. The relationship between discharge capacity (mA h/g) and discharge current density (mA/g) of 2-electrode supercapacitor made by M-30 and M-20.

Another thing that should be emphasised is that the electric conductivity or ohmic resistance of porous materials is closely related to their morphologies. Normally, the higher the surface area, the smaller the particle size, the poor conductivity should be. Besides the kinetic factors related to the pore-size distribution of certain materials, electric conductivity is another limiting factor for power density. However, electric conductivity will not influence the energy density. The rate capability levels are observed the intrinsic problem with high-area double layer capacitor of distributed internal pore resistance within the electrode matrix and conduct resistance among particles. The transmission line model used to fit the AC impedance has taken into account the ohmic resistance of a matrix.

It is worth distinguishing the electric conductivity of activated carbon, which is in the solid side of electrode from the ionic conductivity, which relates to the mobility of ions in the liquid side. Establishing double-layer on the surface of a porous electrode includes separation of ions with opposite charges and movement of ions to opposite direction inside the pores of porous material. The mobility of ions inside the porous matrix is responsible for the rate of electrochemical accessibility. Obviously, the movement of ions in smaller pores is more difficult than in larger pores. So, the ionic conductivity inside the matrix of porous material is conceptually different with that in the bulk of electrolyte; the former one cannot be represented by a single resistor; instead, it has to be represented by a network of resistors because the resistance 'distributes' throughout the whole material.

It is also interesting to point out that the surface area of M-30 (2571.2 m^2/g) is significantly higher than that of M-20 (2130 m^2/g), but the gravimetric specific capacitance of M-20 (100 F/g) is larger than M-30 (62.9 F/g). Since the porosity of M-30 has been proved to be easily accessible, it ruled out the possibility of the existence of non-accessible micropores; the only reason that would be responsible for the controversy is the difference of capacitance per unit area (F/cm^2). The difference of surface specific capacitance results from the surface condition, e.g., functional groups attached, crystal orientation, etc. Those surface conditions are normally determined by the process of synthesis and precursors involved.

Petitioner Intel Corp., Ex. 1048
IPR2023-00783

4. Conclusions

The nature of activated carbon that is responsible for its electrochemical performance, especially high-rate discharge performance, as electrodes used in supercapacitors, have been elucidated by examining its pore distribution and fitting of the AC impedance data. The following points are of value to be noted.

(1) Various activated carbon materials are with their unique pore size distribution due to their precursor and treatments.

(2) Electrochemical accessible time to the pore of different size can be obtained from the fitting of AC impedance based on transmission line model. It is in a good agreement with the profile of pore size distribution obtained from nitrogen adsorption experiments.

(3) Those activated carbons with larger percentage of bigger pores are more suitable to high-power supercapacitor applications because it can deliver high energy at high rate, although it may store less total energy.

(4) Pore size distribution is one of the key factors that dictate the selection of activate carbon material for EDLCs.

References

[1] J. Miller, Double-layer capacitors and related devices, in: S. Wolsky, N. Marincic (Eds.), Proceedings Third International Symposium, Florida Educational Seminars, Boca Raton, FL, 1993.
[2] A. Burk, Double-layer capacitors and related devices, in: S. Wolsky, N. Marincic (Eds.), Proceedings Second International Symposium, Florida Educational Seminars, Boca Raton, FL, 1992.
[3] B.E. Conway, Proceedings Electrochemical Society Symposium on Electrochemical Capacitors, Chicago, IL, USA, Proc. Vol. 95-2, Electrochem. Soc., Pennington, NJ, USA, 1996.
[4] S.T. Mayer, R.W. Petala, J.L. Koschmitter, J. Electrochem. Soc. 140 (1993) 446.
[5] A. Nishino, J. Power Source 60 (1996) 137.
[6] A. Yoshida, S. Nonaka, I. Aoki, A. Nishino, J. Power Source 60 (1996) 2137.
[7] S. Sarangapani, P. Lessner, J. Forchione, A. Griffith, A.B. Laconti, J. Power Source 29 (1990) 355.
[8] T.C. Murphy, G.H. Cole, P.B. Davis, Double-layer capacitors and related devices, in: S. Wolsky, N. Marincic (Eds.), Proceedings Fifth International Symposium. Florida Educational Seminars, Boca Raton, FL, 1995.
[9] J.R. Jow, Double-layer capacitors and related devices, in: S. Wolsky, N. Marincic (Eds.), Proceedings Third International Symposium. Florida Educational Seminars, Boca Raton, FL, 1992.
[10] J.R. Jow, J. Power Source 62 (1996) 155.
[11] NEC Publication, Document No CEP-1004G.
[12] H. Von. Helmhoz, Ann. Phys. 29 (1879) 337.
[13] G. Gouy, J. Phys. 9 (1910) 457.
[14] G. Gouy, Compt. Rend. 149 (1910) 654.
[15] D.L. Chapman, Philos. Mag. 25 (1913) 475.
[16] O. Stern, Z. Elektochem. 30 (1924) 508.
[17] B.E. Conway, Theory and Principles of Electrode Processes, Ronald Press, 1965.
[18] B.E. Conway, W.G. Pell, T.C. Liu, J. Power Source 65 (1997) 53.
[19] B.E. Conway, J. Electrochem. Soc. 138 (1991) 1539.
[20] R.A. Huggins, Mat. Res. Soc. Symp. Proc. Vol. 369, Mater. Res. Soc., Boston, p. 3.
[21] M.M. Thackery, A. de Kock, M.H. Rossouw, D. Liles, R. Bittihn, D. Hoge, J. Electrochem. Soc. 139 (1992) 363.
[22] W. Li, W.R. McKinnon, J.R. Dahn, J. Electrochem. Soc. 141 (1994) 2310.
[23] B.E. Conway, Double-layer capacitors and related devices, in: S. Wolsky, N. Marincic (Eds.), Proceedings Fourth International Symposium. Florida Educational Seminars, Boca Raton, FL, 1994.
[24] S.J. Gregg, K.S.W. Sing, Adsorption, Surface Area and Porosity, Academic Press, London, 1982.
[25] A. Soffer, M. Folman, J. Electroanal. Chem. 25 (1972) 38.
[26] J. Koresh, A. Soffer, J. Electrochem. Soc. 124 (1977) 711.
[27] J. Koresh, A. Soffer, J. Electroanal.Chem. 147 (1983) 223.
[28] Hang Shi, Electrochim. Acta 41 (1996) 1633.

Petitioner Intel Corp., Ex. 1048
IPR2023-00783